AIMS Materials Science, 4(2): 277-291.
DOI: 10.3934/matersci.2017.2.277
Received: 23 October 2016
Accepted: 23 January 2017
Published: 08 February 2017

http://www.aimspress.com/journal/Materials

Research article

Elastic-plastic defect interaction in (a)symmetrical double edge notched tension specimens

Kaveh Samadian *, Stijn Hertelé, and Wim De Waele

Ghent University, Department of Electrical Energy, Metals, Mechanical Construction and Systems Soete Laboratory, Technologiepark 903, 9052 Zwijnaarde, Belgium

* **Correspondence:** Email: Kaveh.Samadian@Ugent.be; Tel: +32-9331-04-80; Fax: +32-9331-04-90.

Abstract: Interaction of defects tends to intensify their crack driving force response compared to the situation where these defects act independently. The interaction between multiple defects is addressed in engineering critical assessment standards like BS7910 and ASME B&PV Section XI. Nonetheless, the accuracy of these rules is open to debate since all of them are based on re-characterization procedures which in essence introduce conservativeness. The authors have developed a fully parametric finite element (FE) model able to generate multiple notches in different topologies, in order to investigate their interaction effect. An experimental validation study is conducted to verify the FE model in terms of CTOD response and surface strain distribution. To that end, symmetrically and asymmetrically double edge notched tension specimens are tensile tested and their deformation monitored by means of 3D digital image correlation. In this study the CTOD is opted as a local criterion to evaluate the interaction between notches. These results are compared with an evaluation of strain patterns on a specimen's surface, as a global interaction evaluation. Through this comparison a deeper understanding is gained to allow us to develop a novel approach to address flaw interaction. Moreover, the validation of the FE model allows future studies of interaction between other defect types (e.g., semi-elliptical, surface breaking) in plate-like geometries.

Keywords: CTOD; interaction; elastic-plastic fracture mechanics; DENT; DIC

1. Introduction

Where two or more adjacent defects are observed in engineering structures such as pressure vessels or pipelines, an evaluation of their interaction is part of the integrity analysis. Under the influence of an applied load, a small (and acceptable) defect can grow and coalesce with a closely distanced adjacent defect. The interaction between defects in case of stress corrosion cracking, fatigue and severe plastic loading plays a dominant role in fracture behavior [1–4]. It should be taken into consideration that defects may occur in different locations with different shapes, and not necessarily in the same plane. Therefore, a sound identification of defect interaction is far from straightforward.

Defects in thin-walled structures can be categorized as embedded, surface-breaking and through-thickness. Even though various standards and guidelines are slightly different in addressing the adjacent flaws, in general the following steps are considered to assess multiple defects. Defects in different cross sections are checked with alignment and re-characterization criteria. Alignment rules are a set of procedures to convert multiple non co-planar defects into co-planar defects. Re-characterization rules convert an embedded defect into a surface defect which is more amenable to analysis. Subsequently, co-planar defects are checked using defect interaction criteria, and if satisfied the defects are combined into a single virtual defect. These interaction criteria can be related to defect length, defect depth and spacing between the defects. It is not necessary to consider further interaction of a combined defect with neighboring defects. This assessment approach has been included in codes and standards such as references [5–8]. Although the majority of these documents have been updated in the last decade to address the issue more accurately, some shortcomings are still observed which may result in overly conservative and in some cases non-conservative assessments [9].

Recently there have been some specific studies regarding the interaction of non-aligned defects. Hasegawa et al. [10] studied alignment rules in stainless steel pipes with multiple non-aligned flaws through series of experiments. It was shown that applying the alignment rules based on the proportion of flaw length, as in most Fitness-For-Service codes, gives a conservative assessment. Kamaya et al. [3,11,12] studied the growth behavior of multiple surface cracks under static and fatigue loads with numerical and experimental methods. While early studies focused on Stress Intensity Factor (SIF), in their recent studies Hasegawa et al. [13] Suga et al. [14,15], Iwamatsu et al. [16,17] and Miyazaki et al. [18] studied numerically and experimentally the plastic collapse behavior in multi-flawed specimens in quasi static bending tests.

J-integral and crack tip opening displacement (CTOD) have been suggested to evaluate the fracture behavior of ductile material [19]. Nonetheless, few researchers used either CTOD or J-integral to evaluate defect interaction. Chang and Kotousov [20] studied the relation of plastic zone size and CTOD for two collinear cracks analytically. Zhang et al. [21] studied fracture response of a pipeline containing two coplanar defects subject to axial straining and internal pressure using CTOD-strain diagrams through 3D finite element simulations. De Waele et al. [22] and De Waele [23] studied flaw interaction behavior for ductile material and highlighted the inconsistency and over conservativism of codes in assessing flaw interaction. They proposed a new criterion based on defect length limit ensuring remote yielding which allows less conservative assessments. Tang et al. [4] proposed a novel flaw interaction rule for pipelines in a strain based design context using the CTOD

as a crack driving force measure. They studied the effect of defect interaction on pipe tensile capacity through both numerical and experimental testing.

While the Fitness-For-Service codes were developed based on linear elastic fracture mechanics (LEFM) there are few researches that study flaw interaction considering elastic-plastic behavior through both numerical and experimental studies. Flaw interaction can be evaluated in different ways; there is an obvious effect on the local response at the defect tip (e.g., crack driving force) which is used in most of the present FFS guidelines. Further, flaw interaction may be reflected in the global deformation behavior of the component. The objective of this study is to verify the applicability of local and global behavior studies for interaction through both numerical and experimental analysis in an elastic-plastic framework. With this fundamental perspective in mind, the present work focuses on the effect of out-of-plane distance between notches in symmetrically Double Edge Notched Tensile (DENT) specimens. Experimental tests are supported by full-field strain measurements aiming to visualize the global deformation behavior. The experiments were designed to gain a basic understanding of strain patterns between the adjacent flaws as well as to measure the crack mouth opening displacement (CMOD) and CTOD locally at each notch. The test results are used to validate a generic finite element model, which has a higher potential to perform parametric studies. Different methods are explored to evaluate defect interaction.

2. Materials and Method

2.1. Specimens and Material

In this work, three specimens having a cross section of 30 mm by 15 mm have been tested, each having different notch out-of-plane distances *S* while having the same notch depth, Figure 1. The notch distances are 0 mm (symmetrical DENT), 30 mm and 45 mm (asymmetrical DENT). The notches were applied by fine saw-cutting, producing an initial notch tip radius equal to 0.075 mm. Fatigue pre-cracking is not applied since this may complicate the control of the initial crack depth and according to previous studies this is not required in materials with sufficient ductility [24,25]. In single edge notched tensile (SENT) test procedures *10W* is typically suggested for minimum daylight length, while in DENT specimens an out-of-plane distance between the flaws should be considered. Therefore, to have a constant length in all specimens, *14W* is selected for daylight length. Table 1 shows an overview of the specimens' dimensions. The specimens have been extracted from API-5L X70 pipeline steel. The specimens are oriented in the L-T direction with respect to the pipe axis (refer to ASTM 1823 [26]). The material 0.2% proof stress is 479 MPa, its tensile strength is 625 MPa and its uniform elongation is equal to 8.0% (as measured using full-thickness prismatic specimens oriented longitudinally to the DENT specimen).

Table 1. Specimens' dimensions.

Specimen	Width (2W)	Thickness (B)	Total length (L)	Daylight length (H)	Out-of-plane notch Distance (S)	Notch No.1 depth (a_1)	Notch No.2 depth (a_2)
DENT0	30 mm	15 mm	300 mm	210 mm	0 mm	6 mm	6 mm
DENT30	30 mm	15 mm	300 mm	210 mm	30 mm	6 mm	6 mm
DENT45	30 mm	15 mm	300 mm	210 mm	45 mm	6 mm	6 mm

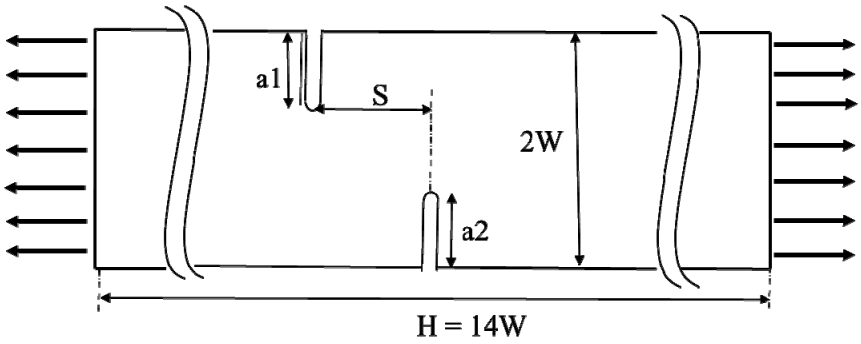

Figure 1. Schematic view of an asymmetrical DENT test specimen.

2.2. Test Procedure

The specimens were clamped using hydraulic grips and loaded in constant displacement rate mode (0.02 mm/sec). The DENT tests were conducted beyond the maximum force in the load-displacement curve and, in order to reach to a sufficient crack extension, till the force dropped back to 80% of its maximum.

In an attempt to capture full field surface deformation and strain during the test, all specimens were analyzed by means of 3D digital image correlation (DIC).

Pictures were obtained from a system provided by Limess Messtechnic & Software GmbH consisting of two synchronized monochromatic 14 bit cameras with a resolution of 2452 by 2054 pixels (5 Megapixels), and analyzed using the VIC3D software (version 7.2.4) supplied by Correlated Solutions Inc. To facilitate accurate DIC analyses, a layer of thin white elastic paint was applied to the frontal surface shown in Figure 1, and subsequently covered with a random pattern of black speckles. The procedure was optimized to obtain high-contrast speckles with a rough size of 3 by 3 pixels, as advised by [27].

Figure 2a shows the clamped symmetrical DENT specimen with speckle pattern and clip gauge, the DIC setup is schematically shown in Figure 2b.

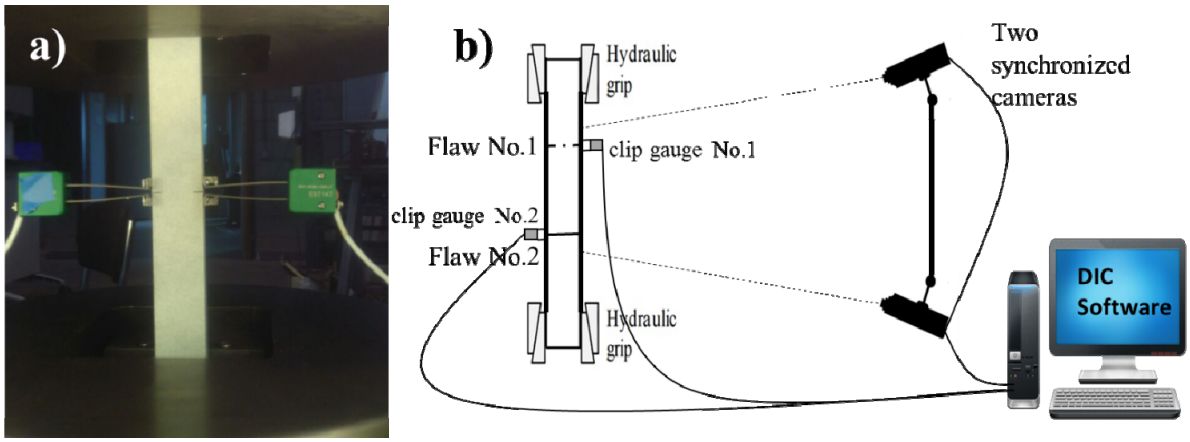

Figure 2. a) Clip gauge position in symmetrical DENT specimen. b) Schematic of the clip gauges and DIC setup.

3. Finite Element Procedure

In an attempt to investigate stress-strain distributions and local behavior of interacting defects, a model containing two through thickness edge notches has been developed by using the finite element software package ABAQUS® version 6.13. In this section, the structure of this model is described. The finite element model is tailored to use an in-house developed full parametric Python script in order to generate various geometries defined by their length (*H*), width (*2W*) and thickness (*B*) containing two (or more) notches characterized by their depth to half width ratio (*a/W*). The notch tips are initially blunted as a previous study showed that notches with 0.075 mm radius (similar to the experimental procedure) behave similar to infinitely sharp cracks upon the development of considerable plasticity (i.e., blunting) in ductile material [24]. To comply with the clamped boundary conditions of DENT tests, the modeled specimen is connected to two rigid bodies at both ends. One end is fixed, and the other is translated under displacement control (rotation is restricted). The specimen cross section is *2WB* and daylight grip length *L* equal to *14W*. An example view of the model showing a configuration with two asymmetrical notches, as particularly considered for this study, is shown in Figure 3a.

Using a parametric Python scripting framework, regular spider web meshes consisting of eight-node linear brick elements with reduced integration scheme (ABAQUS® type C3D8R) are generated in the vicinity of the notch tips. The half circle representing a notch tip consists of 40 elements each having a radial dimension equal to 5.8 μm (around 8% of the notch radius). Multiple flaws in various locations can be simulated and in total the models contain between 62000 and 64000 elements. A mesh convergence study assured a satisfactory numerical accuracy within acceptable computational time. The model is simulated with symmetric boundary conditions in thickness direction for the sake of computational effort and time. In addition, with the aim to obtain realistic deformation patterns in the specimen (including localized necking), a finite strain deformation has been used for all the simulations by applying the NLGEOM option which considers the effect of geometrical non-linearity due to large deformation [28,29]. The stress-strain behavior of the material was implemented on a table with experimentally determined data pairs of stress and the corresponding strain, Figure 3b shows this stress-strain curve. An incremental J2 plasticity scheme is also used which adopts isotropic hardening and the von Mises yield criterion.

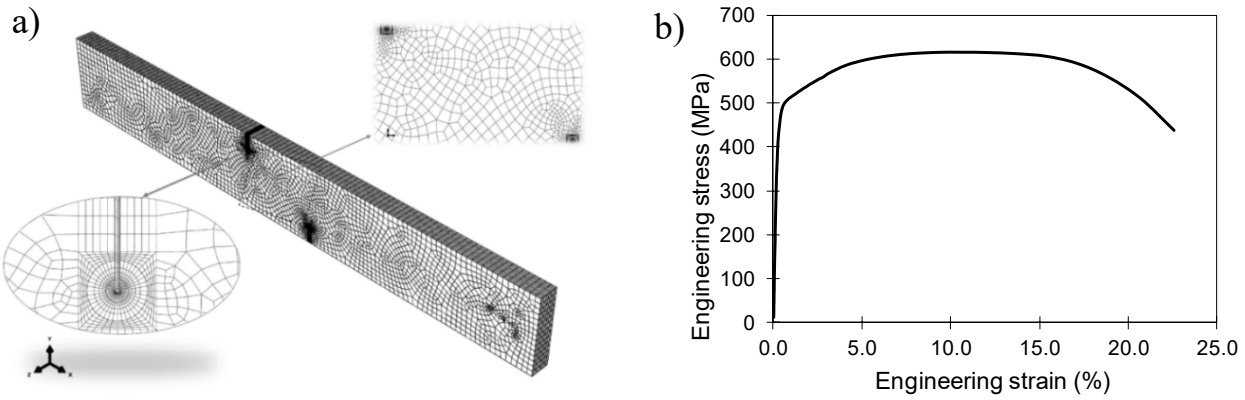

Figure 3. a) Finite Element model, b) Experimentally determined stress-strain curve which is used for material properties in FE model.

For modelling the notch, the stationary crack approach is opted in this study. In this approach, ductile tearing is not implemented and the simulated cracks simply blunt out. Therefore, the FE model validity is up to the crack initiation which is assumed to start when maximum force is reached. As a consequence, the agreement between experimental results and model predictions is expected to vanish beyond the point of stable crack initiation. The main output of the FE model is CTOD, which is obtained through calculation of node displacements around the notch tip and reported as a function of remote stress level.

4. Results

4.1. DIC Verification

In the present study, the CTOD value is used as the main criterion to evaluate interaction as well as verifying the FE model. The CTOD value is measured based on the δ5 definition introduced by GKSS [30] and DIC data are used to extract the displacements around the notch tip according to this definition. In order to verify the DIC measurements, crack opening displacement (COD) has been evaluated since this parameter can be directly measured with clip gauges.

Clip gauges are mounted on two knifes with 2 mm height above the specimen's edges, whereas the measurable zone for DIC starts around 1 mm away from the specimen edge. Assuming straight notch flanks, two lines at both sides of the notch starting at 4 mm below the edge and ending at 1 mm below the edge (the boundary of measurable zone) are assumed; subsequently, the lines are extrapolated for another 3 mm till the top of the knifes (two dashed red lines in Figure 4). Then assuming that triangles A and B in Figure 4 are equal, U_{+2} (representing COD) can be calculated according to equation 1 and this value is compared with clip gauges' readings. Using the same principles and basic trigonometry, CMOD could be calculated based on the same principles as well (equation 2).

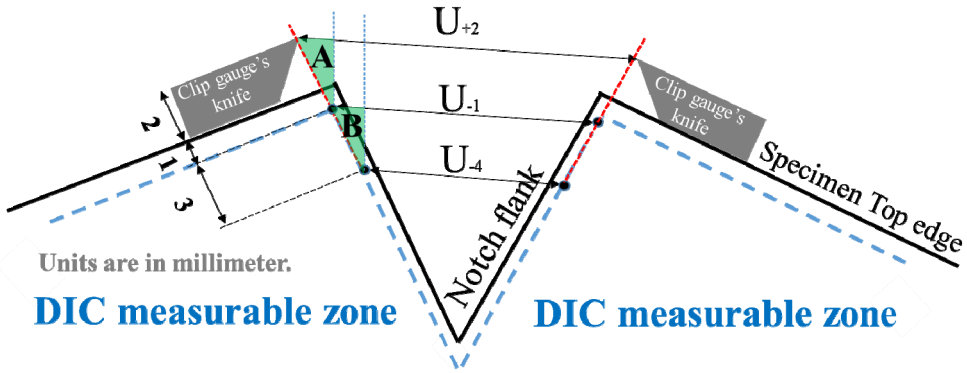

Figure 4. Geometrical assumption used for COD calculation based on DIC measurements.

$$\text{COD} = U_{+2} = 2 \times U_{-1} - U_{-4} \tag{1}$$

$$\text{CMOD} = \frac{4 \times U_{-1} - U_{-4}}{3} \tag{2}$$

Figure 5 shows the comparison of U_{+2} calculated based on equation 1 using DIC measurements and the same value measured directly by clip gauges for all specimens. DENT30 and DENT45 shown an almost perfect 1:1 agreement over the entire measurement range. However, In DENT0 a divergence is noted between both methods with increasing U_{+2}. The same trend was observed in CMOD by Weeks et al. in SENT specimen [31]. This slightly diverging error in DENT0 with increasing CMOD can be explained by possible effects of plastic strains around the notches which affect the obtained displacements through DIC (i.e., U_{-1} and U_{-4}).

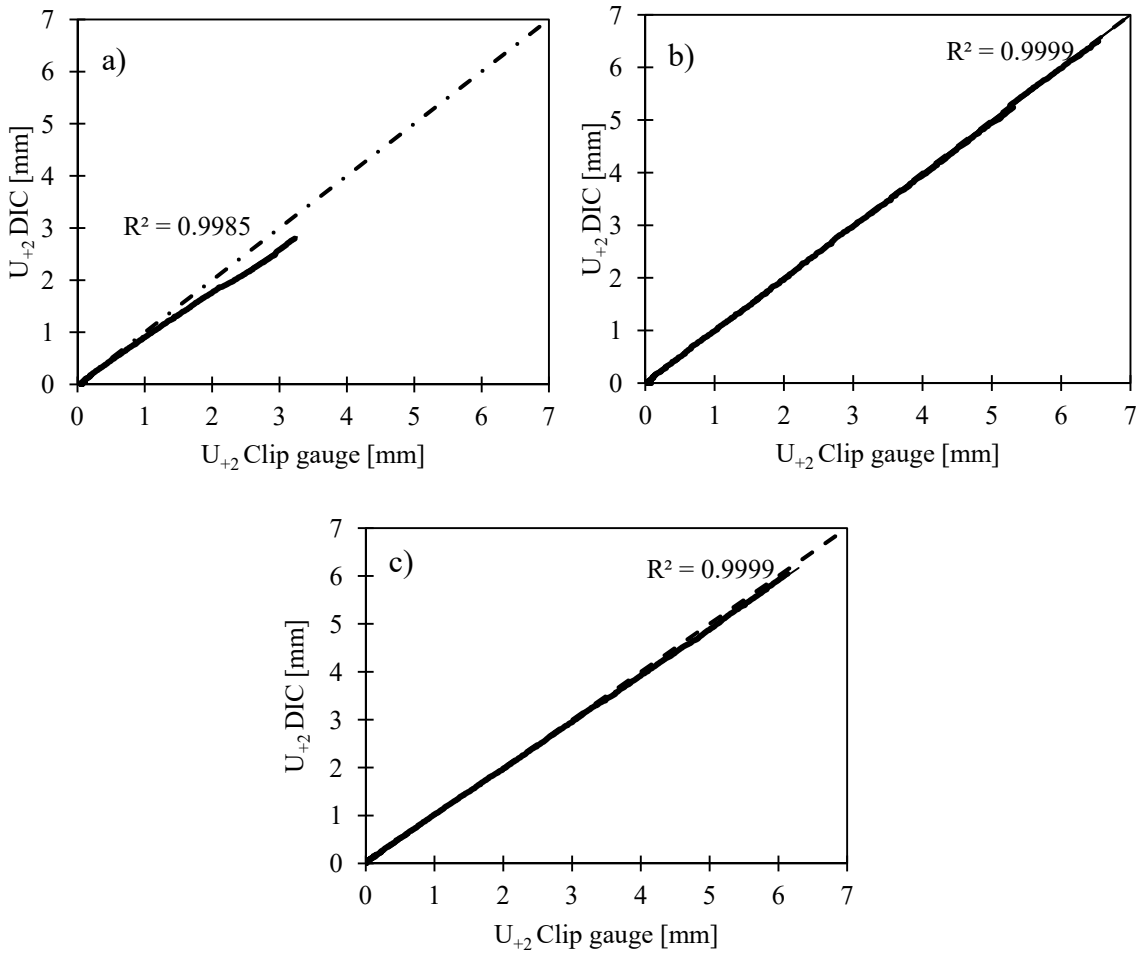

Figure 5. Plot of clip gauge measured COD vs. COD from DIC: a) DENT0, b) DENT30, c) DENT45.

4.2. FEM Verification and Analysis

The FE modelling approach needs experimental validation. In this study, the CTOD versus remote stress (load divided by un-notched cross section) response has been opted to verify the model. CTOD and remote stress were chosen because they are unaffected by the compliance of the universal test rig and because both are relevant with respect to a fracture mechanics analysis. Figure 6 shows comparisons between experimental results of CTOD (measured as δ5 by DIC) versus remote stress with stress normalized against yield strength. The developed model uses a stationary crack approach

(i.e., crack growth is not accounted for). Therefore, upon ductile crack initiation, the normalized stress in experimental graphs dropped after maximum load point and therefore, since the model is not valid after crack initiation, FEM graphs are stopped that point. As apparent from Figure 6, in all experimental specimens, one flaw eventually opens as reflected in its dominating CTOD. The satisfactory agreement reported in Figure 5 for initial yielding (i.e., prior to ductile tearing) is accepted as a first verification of the finite element model.

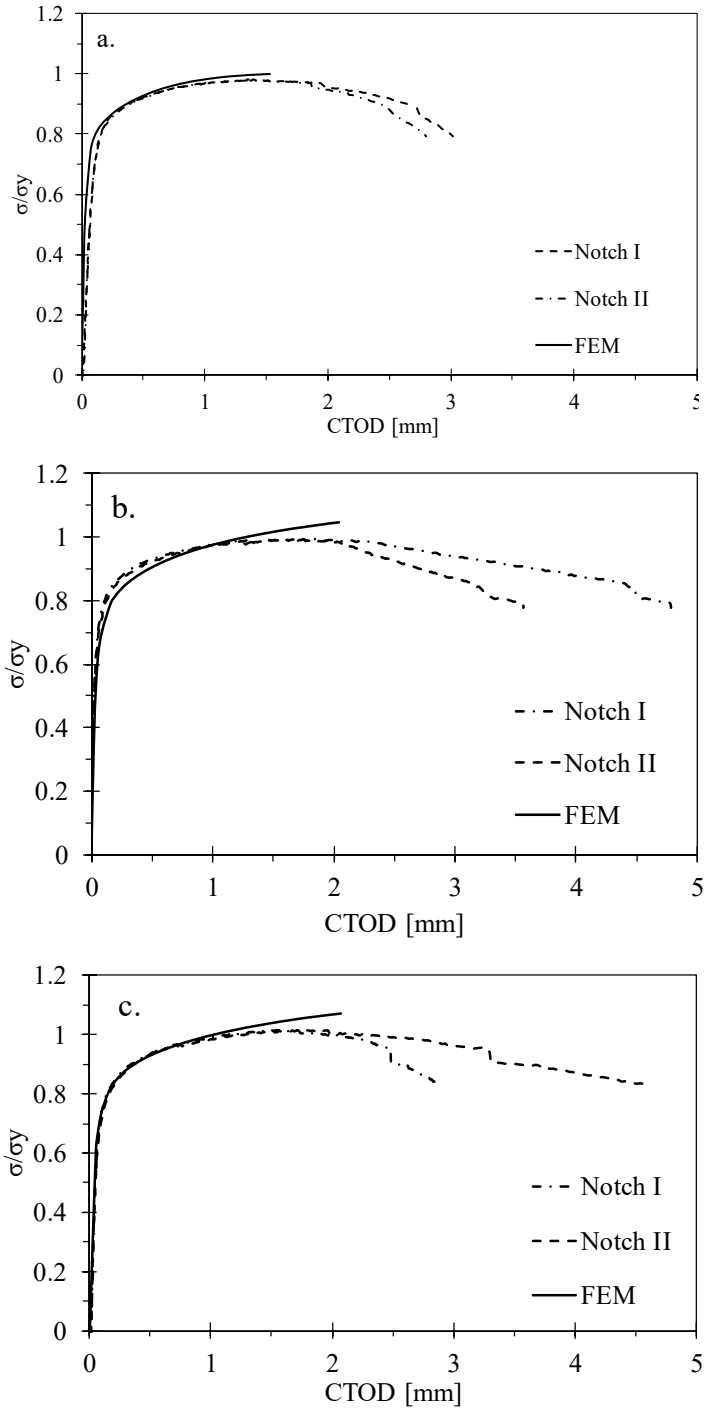

Figure 6. CTOD versus normalized remote stress verification graphs: a) DENT0, b) DENT30, c) DENT45.

The fracture responses are represented by the CTOD values gained from FE models at normalized remote stress levels from 0.8 to 1.0. The upper graph in Figure 7 ($\sigma/\sigma_y = 1$) is plotted for simulations with out-of-plane distance of 20 mm and more since, for the other configurations, early necking prevented remote normalized stress to reach unity. This graph demonstrates the effect of out-of-plane notch distance on CTOD while the flaw's depth and shape were kept constant. It is assumed that when the CTOD value becomes significantly greater than a reference value there is an interaction. The CTOD of a single edge notched tension specimen with identical thickness, width and the crack depth is assumed as the reference value in this paper. A 10% increase in CTOD is assumed as significant, hence, the critical line corresponds to 110% of the CTOD value of the single edge notched specimen. A similar difference was concluded as a threshold to detect interaction between non-planar flaws in previous research using J-integral [9], and since J and CTOD can be converted to each other, the same threshold is applied in this paper.

In Figure 7, the measured CTOD for DENT30 and DENT45 experiments are also reported at four normalized stress levels from 0.8 to 1.0. For DENT0, the experimental CTOD is only reported at normalized stress from 0.80 to 0.95 since this normalized stress value did not reach unity during the experiment.

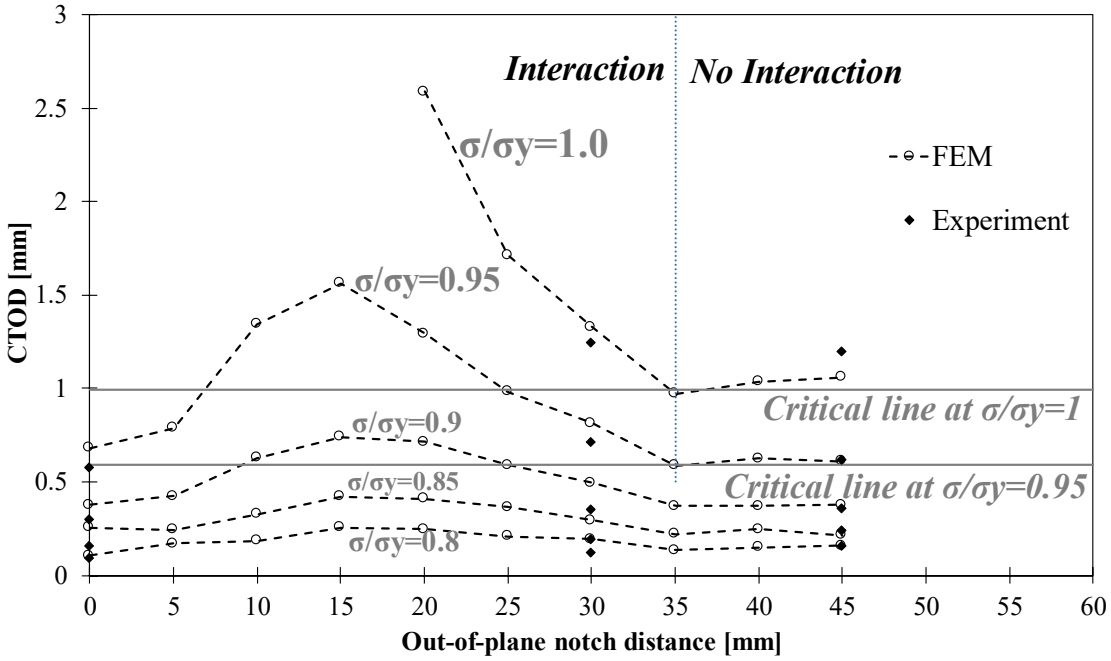

Figure 7. CTOD versus out-of-plane notch distance.

4.3. Strain Patterns

Notch interaction is not only studied through their local behavior (i.e., CTOD), but also through their global behavior as reflected in the strain patterns. Fagerholt et al. [32] used the effective strain concept, equation 3, to assess the strain patterns. The same procedure is applied in this study.

$$\varepsilon_{eff} = \sqrt{\frac{2}{3}(\varepsilon_1^2 + \varepsilon_2^2 + \varepsilon_3^2)} = \sqrt{\frac{4}{3}(\varepsilon_1^2 + \varepsilon_1\varepsilon_2 + \varepsilon_2^2)} \quad (3)$$

where ε_1, ε_2, ε_3 are principal logarithmic strains. The second equality is obtained by assuming incompressibility, for which the out-of-plane strain $\varepsilon_3 = -(\varepsilon_1 + \varepsilon_2)$. The principal strains ε_1 and ε_2 are obtained by DIC.

In Figure 8, the effective strain patterns of the three specimens are shown at three different stages during the test: 1. at an early stage when the pattern starts to appear, 2. when the maximum force is reached, 3. at the end of the test, when force dropped back to 80% of the maximum load.

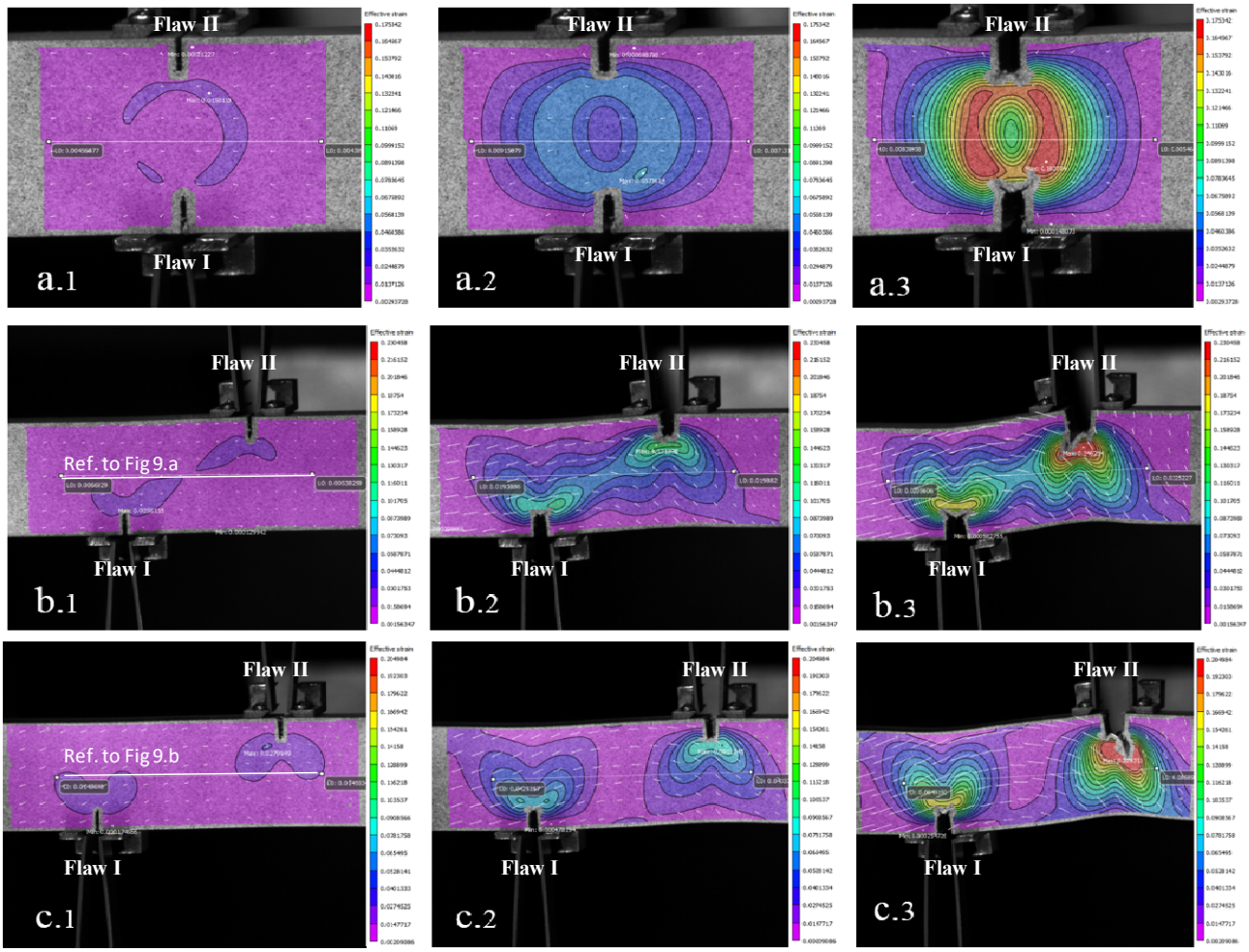

Figure 8. Effective strain pattern graphs: a) DENT0, b) DENT30, c) DENT45. 1) At the early stages of the test, 2) When maximum force is reached, 3) When the force dropped to 80% of its maximum.

In Figure 8, it can be observed that in DENT0 from the onset of loading symmetrical strain patterns were generated around both notches and this continued till the end of loading. As expected both notches have almost equal surrounding strain patterns. In DENT30, the strain patterns clearly tended to interact from the beginning which resulted in non-symmetrical strain pattern development. Crack growth of notch II was observed towards notch I. In DENT45 interaction between strain patterns did not occur from the beginning and patterns developed quite separately. Notch II did not grow towards notch I; considering symmetrical strain patterns around both notches the orientation of crack extension is expected to be arbitrary. A horizontal path was defined at mid-width of the

specimen (as illustrated in Figure 8), along which effective strain evolutions were assessed (Figure 9). The horizontal axis shows the distance along the midline path. The vertical axis shows the effective strain and graphs are plotted for different remote strain values during the test. The FE results in Figure 9 are reported at a normalized remote stress (σ/σ_y) equal to 1. While different gray values demonstrate various stages of the test (darker corresponding with more applied deformation), the effective strain pattern at remote normalized stress equal to 1 is highlighted (with the cross marks) in order to compare the experimental results with FE results as well as to emphasize the differences in the patterns before and after the approximate crack growth initiation.

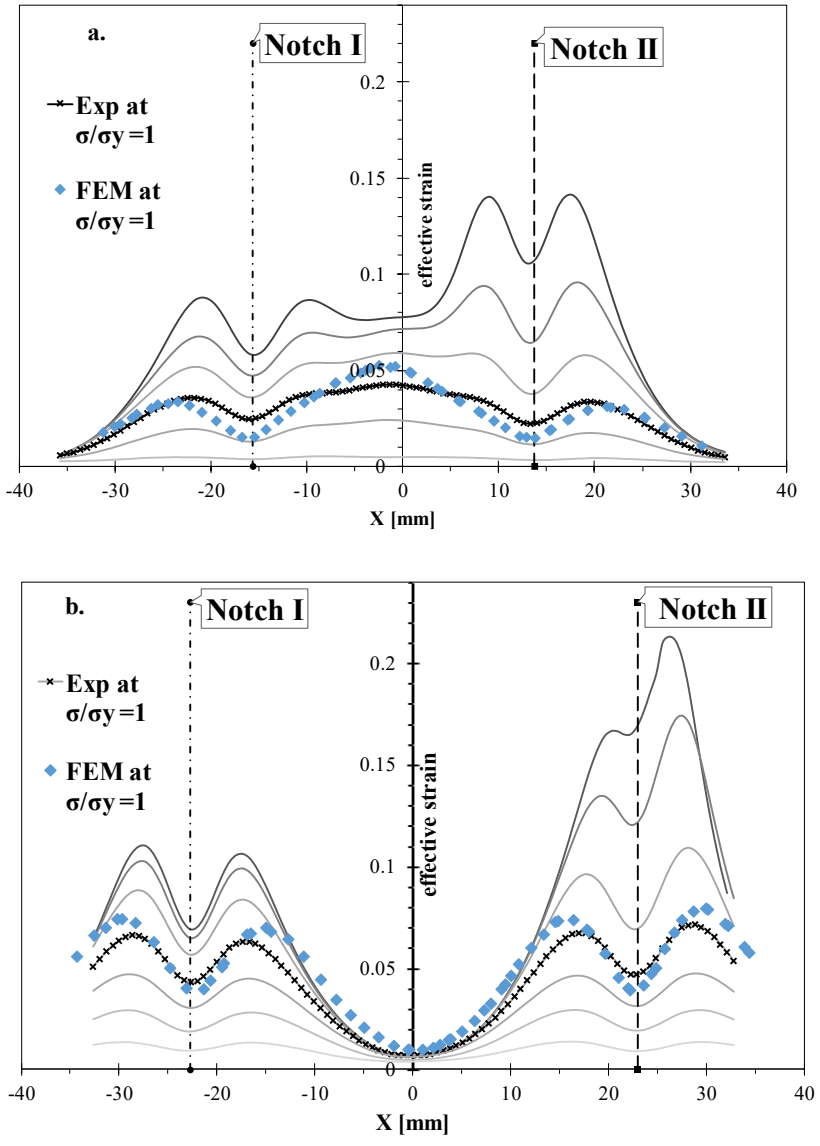

Figure 9. Strain pattern graphs: a) DENT30, b) DENT45.

5. Discussion

The study of CTOD (Figure 7), representative of local behavior at notch tip, reveals that for distances closer than a critical value notches clearly open more than is the case for a single notch.

When the notches are far enough from each other they behave almost similar as an individual notch. The evaluation of CTOD in the interaction zone is represented by a peak (Figure 7). This means that when two identical notches are interacting, the distance between them is not the only parameter defining their local behavior. However, these results need to be interpreted with caution because the proposed magnitude of CTOD may not describe the interaction behavior completely. The trend of CTOD before the peak point for closely located notches can be justified considering the crack tip constraint. Symmetrical DENT, here known as DENT0, is a well-known example of high crack tip constraint. Thus, the constraint enhances stress triaxiality which consequently delays yielding. Therefore, at the point where normalized stress becomes equal to 0.95, the CTOD values of DENT0 and DENT5 are lower than for the other specimens, although the notches are extensively interacting. Increasing the out-of-plane distance to 10 mm, the constraint effect reduces since the notch tips are further distanced. This explains why in DENT15 a peak appears in CTOD value, the interaction between adjacent notches becomes the dominant factor when the constraint effect is negligible.

The symmetrical DENT specimen is not a typical configuration to be considered in flaw interaction criteria. Nonetheless, ASME B&PV XI alignment criteria for non-planar flaws can be compared with the results of DENT simulation. According to ASME, non-planar flaws located in two planes with distance less than 12.5 millimeters should be aligned in the same plane. Therefore, in the present study when the out-of-plane distance of notches becomes less than 12.5 mm interaction presence should be checked and for the notches located beyond this distance ASME does not expect any interaction. Although the 12.5 mm borderline seems non-conservative in comparison to the results illustrated in Figure 7, the conclusion should be made with caution since DENT geometry is not a conventional geometry for codes like ASME B&PV XI. Thus, further studies are required to make a better judgment about the ASME (and other FFS codes) alignment criteria for this type of geometry.

The effective strain patterns illustrated in Figure 8 show that the interaction not only can be identified by local behavior (i.e., CTOD) but also can be observed in global behavior around the flaws. Referring to Figure 7, interaction is assumed for less than 35 mm distance between two flaws. As highlighted in Figure 8, there are considerable differences in strain patterns between the DENT30 (which is inside the interaction zone) and DENT45 (which is outside the interaction zone) specimens. The same differences are apparent in Figure 9, where for DENT45 (subfigure b) the effective strain evolutions around both notches are independent and almost equal (till maximum load). From this point on a crack may start to grow which makes the strain pattern asymmetric. The strain evolution in the region between both notches remains unaffected by the notch deformations. It can therefore be assumed that the notches do not interact. Figure 9b shows that, although the FE model tends to over predict the strains in the vicinity of notch tips, the general trend of strains can be reasonably predicted by the model. For DENT30 (Figure 9a) strain concentration appears in between the two notches from the beginning of the test. This reveals that both notches are interacting. Beyond maximum load the strain concentration is most pronounced around one of the notches. However, the effective strain in between both notches is also further increasing. This clearly demonstrates that both notches are indeed interacting. The FE result in Figure 9a also shows higher strains in comparison to the experiment, and since the notches are closer to each other in DENT30 compared to DENT45, higher strains around the notches superimpose with each other. Nonetheless, the same conclusion for determining the interaction can be derived by applying either experimental or FE results.

Although the approaches illustrated by Figure 7 (local approach based on CTOD) and Figure 9 (global approach based on effective strain evolution) are different in essence, they lead to a similar evaluation of notch interaction.

6. Conclusion

In this paper, a generic fully parametric FE model is introduced to simulate the notch interaction in (a)symmetric double edged notched specimens. The model is successfully verified through a series of full-field strain analyses and clip gauge measurements. The following is concluded:

1. DIC as a full-field optical strain measurement method is applied adequately in assessing the crack opening displacement and deformation around the notches in (a)symmetrical DENT specimens.
2. Although CTOD is a useful parameter to identify the interaction behavior in DENT geometry, the crack tip constraint also affects the local behavior for distinct distances. This aspect of defect interaction requires further investigation.
3. Global deformation around the notches obtained through DIC measurements can also be applied to study the interaction. Results show that the same conclusion can be drawn by applying either a quantitative criterion based on CTOD or a qualitative study using effective strain patterns.

More efforts are required to quantify the effect of different factors on interaction with the aim to develop a better understanding in terms of local and global behavior.

Acknowledgments

The authors would like to acknowledge the financial supports from Ghent University through grant number BOF13/24J/122.

Conflict of Interest

All authors declare no conflicts of interest in this paper.

References

1. Kamaya M, Haruna T (2006) Crack initiation model for sensitized 304 stainless steel in high temperature water. *Corros Sci* 48: 2442–2456.
2. Yan X (2006) Multiple crack fatigue growth modeling by displacement discontinuity method with crack-tip elements. *Appl Math Model* 30: 489–508.
3. Kamaya M (2008) Growth evaluation of multiple interacting surface cracks. Part II: Growth evaluation of parallel cracks. *Eng Fract Mech* 75: 1350–1366.
4. Tang H, Fairchild DP, Cheng W, et al. (2014) Development of Surface Flaw Interaction Rules for Strain-Based Pipelines. The Twenty-fourth International Ocean and Polar Engineering Conference, 3: 476–486.
5. American Petroleum Insititute (2013) API Standard 1104: Welding of Pipelines and Related Facilities.

6. American Petroleum Institute (2007) API-579-1/ASME FFS-1: Recommended practice for fitness-for-service.
7. British Standards Institute (2015) BS7910:2013+A1:2015: Guide to methods for assessing the acceptability of flaws in metallic structures.
8. American Society of Mechanical Engineers (2010) ASME Boiler and Pressure vessel Code XI: Rules for Inservice Inspection of Nuclear Power Plant Components.
9. Kamaya M (2006) Flaw Proximity Rules for Parallel Surface Cracks Based on Elastic, Elastic-Plastic Fracture Mechanics and Limit Load Analyses. ASME 2006 Pressure Vessels and Piping/ICPVT-11 Conference, 1–8.
10. Hasegawa K, Miyazaki K, Saito K, et al. (2009) Evaluation of alignement rules using stainless steel pipes with non-aligned flaws. ASME 2009 Pressure Vessels and Piping Conference, 1–8.
11. Kamaya M (2003) A Crack Growth Evaluation Method for Interacting Multiple Cracks. *JSME Int J Series A* 46: 15–23.
12. Kamaya M, Masanori Kikuchi EM (2009) Growth Behavior of Two Interacting Surface Cracks of Dissimilar Size. ASME 2009 Pressure Vessels and Piping Conference, 1–5.
13. Hasegawa K, Miyazaki K, Saito K (2010) Behavior of plastic collapse moments for pipes with two non-aligned flaws. ASME 2010 Pressure Vessels and Piping Division/K-PVP Conference, 1–7.
14. Suga K, Miyazaki K, Kawasaki S, et al. (2011) Study On Interaction of Multiple Flaws in Ductile Fracture Process. ASME 2011 Pressure Vessels and Piping Conference.
15. Suga K, Miyazaki K, Senda R, et al. (2012) Interaction Efect Evaluation of Plural Surface Cracks in Ductile fracture Process. ASME 2012 Pressure Vessels and Piping Conference, 1–6.
16. Iwamatsu F, Miyazaki K, Saito K, et al. (2009) Experimental Estimation of Fully Plastic Collapse Stresses for Pipes with Three Circumferential Flaws Fuminori. ASME 2009 Pressure Vessels and Piping Conference, 1–5.
17. Iwamatsu F, Miyazaki K, Takazawa H, et al. (2013) Evaluation Procedure of Limit Load for Non-aligned Multiple Flaws. ASME 2013 Pressure Vessels and Piping Conference, 1–6.
18. Miyazaki K (2011) Effect of flaw dimensions on ductile fracture behavior of non-aligned multiple flaws in a plate. ASME 2011 Pressure Vessels and Piping Conference.
19. Hutchinson JW (1983) Fundamentals of the Phenomenological Theory of Nonlinear Fracture Mechanics. *J Appl Mech* 50: 1042.
20. Chang D, Kotousov A (2012) A strip yield model for two collinear cracks in plates of arbitrary thickness. *Int J Fract* 176: 39–47.
21. Zhang YM, Ariffin MZ, Xiao ZM, et al. (2015) Nonlinear elastic-plastic stress investigation for two interacting 3-D cracks in offshore pipelines. *Fatigue Fract Eng M* 38: 540–550.
22. De Waele W, Denys Rudi, Lefevre A (2006) Development of defect interaction criteria for pipeline girth welds subjected to plastic collapese conditions. ASME 2006 Pressure Vessels and Piping/ICPVT-11 Conference.
23. De Waele W (2005) The Interaction of Weld Defects under Plastic Collapse. *Mater Sci Forum* 475: 2735–2738.
24. Verstraete MA, Hertelé S, Denys RM, et al. (2014) Evaluation and interpretation of ductile crack extension in SENT specimens using unloading compliance technique. *Eng Fract Mech* 115: 190–203.

25. Exxonmobil (2010) Measurement of Crack-Tip Opening Displacement (CTOD) Fracture Resistance Curves Using Single-Edge Notched Tension (SENT) Specimens.
26. ASTM International (2003) ASTM E1823-96: Standard Terminology Relating to Fatigue and Fracture Testing.
27. Sutton MA, Deng X, Ma F, et al. (2000) Development and application of a crack tip opening displacement-based mixed mode fracture criterion. *Int J Solids Struct* 37: 3591–3618.
28. Kim NH (2015) *Introduction to Nonlinear Finite Element Analysis*, New York: Springer.
29. Abaqus Documentation 6.13 (2013) Dassault Systèmes Simulia Corp., Providence, RI, USA.
30. Schwalbe KH, Heerens J, Zerbst U, et al. (2002) GKSS test procedure for determining the fracture behaviour of materials (GKSS 2002/24). Geesthacht: GKSS-Forschungszentrum Geesthacht GmbH.
31. Weeks TS, Sowards JW, Rentz RA, et al. (2016) Comparison of J-intergal Measurment Method on Clamped Single-Edge Notched Tension Specimens. 2016 11th International Pipeline Conference, 1–11.
32. Fagerholt E, Østby E, Børvik T, et al. (2012) Investigation of fracture in small-scale SENT tests of a welded X80 pipeline steel using Digital Image Correlation with node splitting. *Eng Fract Mech* 96: 276–293.

AIMS Press